Effects of Gonadal Hormones On Glutamatergic Circuits in the Retina

Mahito Ohkuma
Fujita Health University
Takuma Maruyama
Nippon Medical School
Toshiyuki Ishii
Nippon Medical School
Nozomi Igarashi
Tokyo University
Keiko Azuma
Tokyo University
Tatsuya Inoue
Yokohama City University
Ryo Obata
Tokyo University
Ei-ichi Miyachi
Fujita Health University
Makoto Kaneda (mkaneda@nms.ac.jp)
Nippon Medical School

Research Article

Keywords: retina, glutamate, mouse, imaging

Posted Date: October 25th, 2021

DOI: https://doi.org/10.21203/rs.3.rs-967890/v1

Abstract

Gonadal hormones function as neurosteroids in the retina; however, their targets in the retina have not yet been identified. The present study examined the effects of gonadal hormones on glutamatergic circuits in the retina. Extracellular glutamate concentrations, which correspond to the amount of glutamate released, were monitored using an enzyme-linked fluorescent assay system. Progesterone and pregnenolone both increased extracellular glutamate concentrations at a physiological concentration in pregnancy, whereas estrogen and testosterone did not. Synaptic level observations using a patch clamp technique revealed that progesterone increased the activity of glutamatergic synapses. We also investigated whether high concentrations of gonadal hormones induced changes in the retina during pregnancy. The present results indicate that progesterone activates glutamatergic circuits as a neurosteroid when its concentration is elevated in pregnancy.

Introduction

Gonadal hormones synthesized in the central nervous system function as neurosteroids [1–4]. They modulate $GABA_A$ and NMDA receptors and contribute to synaptogenesis in the developing brain as well as the differentiation of oligodendrocytes. These hormones also function as neuroprotective and anti-anxiolytic agents. The effects of gonadal hormones as neurosteroids have been investigated at multiple levels in the retina. The presence of receptors for and the synthetic ability of gonadal hormones in the retina have been demonstrated using immunohistochemical methods [5–7]. Furthermore, sex-related differences in retinal function and diseases [8–10] as well as estrus cycle-dependent changes in ocular function [11–14] have been reported. Based on these biophysiological findings, the therapeutic application of gonadal hormones to the treatment of retinal diseases has been examined. The neuroprotective effects of progesterone may be useful for the treatment of retinitis pigmentosa [15–23]. Similarly, estrogen-induced increases in retinal blood flow [24] may be beneficial for neuroprotection [25]. Increases in the thickness of the choroid in pregnancy have frequently been reported [26–30], which may be due to the larger blood volume in pregnancy. In addition, visual changes commonly occur in pregnancy [12–14, 31,32]. The effects of gonadal hormones as neurosteroids in the retina are supported by accumulated evidence; however, their targets have not yet been examined in detail at the cellular level. Furthermore, although changes in retinal thickness in pregnancy have been demonstrated [33,34], a systematic analysis has not been conducted.

Therefore, the present study examined the effects of gonadal hormones in the retina. We investigated whether gonadal hormones modulate the activity of glutamatergic circuits in the retina using an enzyme-linked fluorescent assay system [35] and patch clamp technique. The results obtained revealed that progesterone increased the activity of glutamatergic circuits, whereas estrogen and testosterone did not. We also attempted to establish whether high concentrations of gonadal hormones in pregnancy induce glutamate toxicity in the human retina. Collectively, the present results indicate that progesterone activates glutamatergic circuits without toxic effects when its concentration is elevated in pregnancy.

Results

Effects of gonadal hormones on extracellular glutamate concentrations

Extracellular glutamate concentrations were estimated based on fluorescent intensity measured using the enzyme-linked fluorescent assay system (Fig. 1A). Since fluorescent intensity in the OS contains a significant amount of the intrinsic fluorescent signal of NADH in this system, the signal level in the OS becomes very high [35].

In females, the application of 1 μM progesterone increased the intensity of fluorescent signals (Fig. 1B). In most samples, the intensity of fluorescent signals peaked within 2-4 min and then gradually decreased. We then applied a high K solution to the same samples in order to confirm the viability of samples.

The percent change in signal intensity (dF/F) at individual ROI was calculated using our previously described method [35]. We demonstrated that dF/F in individual layers reflected changes in glutamate concentrations and also that these changes were not limited to the synaptic layers (OPL and IPL) [35]. In females, a significant increase in dF/F was observed in all layers (Fig. 1C). In males, a significant increase in dF/F was not detected in any layers, whereas an increase in dF/F was found in all layers (Fig. 1D).

We then examined the effects of estrogen or testosterone on glutamatergic circuits in females using the enzyme-linked fluorescent assay system. The application of 1 μM 17-β-estradiol increased the intensity of fluorescent signals in all layers (Fig. 2A). However, the increase in dF/F was subtle. The application of 1 μM testosterone did not induce any increase in fluorescent signals in any layers (Fig. 2B).

Since progesterone is synthesized from pregnenolone, we investigated whether pregnenolone mimics the effects of progesterone. The application of 1 μM pregnenolone induced an increase in fluorescent signals in INL, IPL, and GCL (Fig. 2C). We also observed an increase in dF/F in ONL and OPL, whereas that in dF/F was not significant.

Effects of progesterone on EPSCs

We investigated whether progesterone increased the release of glutamate in the retina. To monitor the activity of glutamatergic circuits, we recorded EPSCs from retinal ganglion cells that receive glutamatergic inputs from bipolar cells (Fig. 3A, B, and C). We examined the following six parameters. Frequency and total charge transfer are employed to evaluate the activity of glutamatergic synapses, while the amplitude, decay time, rise time, and charge transfer of individual EPSCs are useful for assessing presynaptic vesicle sizes or the properties of postsynaptic glutamatergic receptors. In the present study, we limited our electrophysiological analysis data to distinguish EPSCs from baseline noise (amplitude >8pA), as described in the Methods section.

In females, progesterone increased the frequency (Fig. 3D, Table 1) and total charge transfer (Fig. 3I, Table 1) of EPSCs. In males, increases in both the frequency (Fig. 3D, Table 1) and total charge transfer

(Fig. 3I, Table 1) were not significant; however, progesterone appeared to affect both parameters. Progesterone increased the charge transfer of individual EPSCs in males (Fig. 3H, Table 1), whereas no significant differences were observed in females (Fig. 3H, Table 1). Furthermore, no significant changes were noted in amplitudes (Fig. 3E, Table 1), rise times (Fig. 3G, Table 1), or decay times (Fig. 3F, Table 1) in males or females.

Table 1
Summary of EPSC analyses

	Parameters	Control (Mean±SD)	Progesterone (Mean±SD)	P value
Female	Frequency (Hz)	19.7 ± 16.2	23.2 ± 19.3	0.032
	Charge transfer of an individual EPSC (pC/event)	0.023 ± 0.008	0.024 ± 0.009	0.458
	Amplitude (pA)	13.1 ± 2.1	13.4 ± 1.9	0.133
	Rise time (ms)	1.135 ± 0.195	1.203 ± 0.192	0.183
	Decay time (ms)	1.47 ± 0.39	1.48 ± 0.46	0.753
	Total charge transfer (pC/30s)	14.7 ± 11.7	17.9 ± 14.5	0.036
Male	Frequency (Hz)	19.7 ± 26.4	23.6 ± 31.5	0.178
	Charge transfer of an individual EPSC (pC/event)	0.020 ± 0.006	0.022 ± 0.007	0.039
	Amplitude (pA)	11.8 ± 1.5	12.1 ± 1.8	0.196
	Rise time (ms)	1.165 ± 0.120	1.191 ± 0.108	0.371
	Decay time (ms)	1.43 ± 0.24	1.51 ± 0.27	0.101
	Total charge transfer (pC/30s)	15.4 ± 27.0	20.4 ± 35.9	0.188
n = 8 (female), n = 9 (male)				

The present results indicate that progesterone increased the frequency of glutamate release from bipolar cell terminals without affecting presynaptic vesicle sizes or the properties of postsynaptic glutamate receptors. In addition, the effects of progesterone were distinct, particularly in females, confirming the results of the enzyme-linked fluorescent assay system.

Changes in retinal thickness during pregnancy

In the present study, we showed that 1 μM progesterone, a nearly maximum concentration in pregnancy [37], activated the glutamatergic circuit of the retina *in vitro*. When extracellular glutamate concentrations are high, glutamate may act as a toxin that induces cell death [41]. Therefore, we examined whether the

elevated concentration of progesterone in pregnancy is associated any morphological changes in the human retina. Since a change in retinal thickness in pregnancy has been reported in age-matched studies [33,34], we monitored retinal thickness during pregnancy to assess morphological changes in the same pregnant women.

In the postpartum stage, progesterone concentrations (43 ± 16 nM, mean ± SD) were within normal values for the regular menstrual cycle (Fig. 4). Rapid elevations in progesterone concentrations during pregnancy were observed in the 1st trimester. The mean concentration of progesterone in the 1st trimester (153 ± 3 nM, mean ± SD) was 2.5-fold that of the highest concentration under the regular menstrual cycle. Progesterone concentrations continued to gradually increase in the 2nd trimester (188 ± 50 nM, mean ± SD) and peaked in the 3rd trimester (243 ± 61 nM, mean ± SD).

We used the thickness of the retina in the postpartum stage as the control because the concentration of progesterone returned to the level of the regular menstrual cycle. We measured the thickness of the retina in 9 regions (Table 2, Fig. 5). Retinal thickness was calculated at the parafovea and perifovea for individuals and averaged (see the Methods section). Significant decreases in thickness were observed in the parafovea and perifovea in the 1st trimester (Fig. 6), but not in the 2nd trimester. In the 3rd trimester, a significant decrease in thickness was only detected in the parafovea.

Table 2
Thickness of the retina in pregnant women

	1st trimester	2nd trimester	3rd trimester	Postpartum
F	258.0 ± 13.2	256.0 ± 12.2	257.6 ± 11.5	257.5 ± 11.3
SPa	339.5 ± 12.6	341.0 ± 11.7	340.6 ± 10.4	342.8 ± 13.0
TPa	322.5 ± 10.1	324.0 ± 10.7	322.7 ± 9.0	325.2 ± 11.0
NPa	339.3 ± 12.6	340.5 ± 10.8	340.4 ± 9.7	342.6 ± 12.5
IPa	334.0 ± 10.6	335.1 ± 11.8	334.8 ± 9.5	337.5 ± 12.1
SPe	302.3 ± 15.5	303.3 ± 15.2	303.7 ± 13.7	303.6 ± 15.6
TPe	285.0 ± 15.5	285.9 ± 15.1	287.6 ± 14.3	288.3 ± 16.6
NPe	318.3 ± 16.4	318.9 ± 16.3	318.7 ± 14.8	320.0 ± 16.1
IPe	288.5 ± 17.0	289.3 ± 17.5	290.5 ± 16.6	291.2 ± 18.0
Data are shown as the mean ± SD.				
F: fovea, Spa: superior parafovea, TPa: temporal parafovea, NPa: nasal parafovea, IPa: inferior parafovea, Spe: superior perifovea, TPe: temporal perifovea, NPe: nasal perifovea, IPe: inferior perifovea				

Discussion

In the present study, we investigated the effects of gonadal hormones on glutamatergic circuits at 1 μM. The results obtained demonstrated that progesterone and pregnenolone increased the activity of glutamatergic circuits at physiological concentrations in pregnancy, whereas neither estrogen nor testosterone modulated the activity of these circuits. In women, progesterone and estrogen concentrations in blood increase and decrease during the menstrual cycle and markedly increase in pregnancy [36]. Under a regular menstrual cycle, the concentrations of progesterone and estrogen fluctuate between 3 and 60 nM and between 0.3 and 1.2 nM, respectively. In pregnancy, the maximum concentrations of both progesterone and estrogen peak at 1 μM [37]. The concentration of testosterone in blood is <35 nM [36]. Therefore, the effects of 1 μM progesterone on glutamatergic circuits may be of physiological relevance.

Regarding the physiological importance of functional changes in the retina, we herein demonstrated that the modulatory effects of progesterone on glutamatergic circuits were stronger in females than in males. In other words, glutamatergic circuits may be more sensitive to progesterone in females than in males. However, no significant differences in the localization or expression of progesterone receptors were reported between male and female mice [23]. Many pregnant women develop physiological alterations in the eye [12–14,30–32]. Among the physiological alterations reported, changes that occur in the visual field may be related to the present results. A change in the visual field was detected as an altered mean threshold sensitivity without subjective symptoms. Although increases in progesterone concentrations in pregnancy may induce functional changes in the retina, these changes may be compensated for through plastic changes in the visual system. Further studies are needed to confirm whether subtle subjective symptoms are present in normal pregnant women.

We observed a detectable reduction in retinal thickness during pregnancy and an elevated extracellular glutamate concentration in the enzyme-linked fluorescent assay system. However, glutamate toxicity is not likely to induce this reduction in retinal thickness for the following reasons. The increase induced in EPSCs by progesterone may elevate the concentration of glutamate at the synaptic cleft. When this elevation persists for a longer time, it may induce glutamate toxicity. However, it is important to note that the increase observed in the extracellular concentration of glutamate in the enzyme-linked fluorescent assay system was detected in the presence of TBOA, an antagonist of glutamate transporters [38]. We previously reported that fluorescence did not increase in the absence of TBOA when a high K stimulation was performed [35], suggesting that glutamate concentrations at the synaptic cleft are tightly controlled by glutamate transporters under physiological conditions. The increase in glutamate release observed in the present study reflects the activation of glutamatergic circuits potentially inducing the subtle functional modulation of visual function [12–14,30–32], but not glutamate toxicity in pregnancy. In the present study, we used retinal thickness in the postpartum period as the control because the progesterone concentration in blood is close to that in the non-pregnant stage. In a previous age-matched study, foveal thickness in the 1st trimester was similar to that in the non-pregnant stage, whereas a significant increase in foveal thickness was detected in the 2nd and 3rd trimesters [33]. If this increase in retinal thickness persists for a few months after delivery, a decrease in retinal thickness may be reconsidered from a different viewpoint.

Alternatively, a temporal decrease in retinal thickness may be explained by increased pressure from the choroid, which becomes thicker due to increased blood flow in pregnancy [26–30]. Further studies are warranted.

We found that progesterone and pregnenolone both increased extracellular glutamate concentrations using the enzyme-linked fluorescent assay system. We also demonstrated that progesterone increased glutamatergic inputs from bipolar cells in retinal ganglion cells. This result indicates that bipolar cells are one of the targets of progesterone. At the immunocytochemical level, the expression of progesterone receptors has been reported in both Müller cells and the pigment epithelium [5] of the mouse retina and Müller cells of the pig retina [6]. In addition, at the immunohistochemical level, immunoreactivity for progesterone receptors was found to be widely distributed, including two synaptic layers (OPL and IPL) [23]. In previous studies, progesterone and pregnenolone were shown to act on TRP channels (TRPM1 [42], TRPM3 [43–45], TRPC6 [46], and TRPM8 [47]), suggesting their stimulation of glutamatergic circuits via the activation of TRP family members. In the retina, TRPM3 is expressed in the inner retina (IPL and GCL) [48] and TRPM1 has been detected in the dendrites of rod bipolar cells [49]. Pregnenolone has been shown to activate TRPM3 and increase Ca influx in the mouse retina [45]. However, TRPM3 channels do not appear to be the target of pregnenolone because progesterone was found to inhibit TRPM3 channels via a pregnenolone-independent mechanism [44]. The activation of TRPM1 by pregnenolone has also been supported in the recombinant system [42]. According to this experiment, the current amplitude of homomeric TRPM1 receptors is very small, while that of chimeric receptors of TRPM1 and TRPM3 is large. Therefore, further studies are needed to establish whether TRPM1 is the actual target of progesterone.

In the present study, we showed that an elevated progesterone concentration in pregnancy may activate glutamatergic circuits at the bipolar cell level in the retina and also that the increased release of glutamate from synaptic terminals may induce subtle changes in vision in pregnancy. Since the retina uses many types of neurotransmitters at multiple synaptic levels, the effects of gonadal hormones on other neural circuits need to be clarified in order to obtain a more detailed understanding of their effects on the retina in pregnancy.

Methods

Approval from Ethical Committees

The experimental procedure for enzyme-linked fluorescence assays on animals was approved by the Institutional Animal Care and Use Committee of Fujita Health University.

The experimental procedure for electrophysiological recordings on animals was approved by the Animal Experiments Ethical Review Committee of Nippon Medical School.

The experimental procedure for the clinical study was approved by the Ethics Committee at the coordinating center of the University of Tokyo and the Institutional Review Board of the University of Tokyo.

All studies were performed in accordance with the relevant guidelines and regulations (for animal studies), and the Declaration of Helsinki. All animal studies were conducted in accordance with the ARRIVE (Animal Research: Reporting of In Vivo Experiments) guidelines.

Experimental procedure for animals

Two techniques were used in the present study to monitor glutamate release from presynaptic terminals in the animal model: an enzyme-linked fluorescent assay system and electrophysiological recordings. We previously demonstrated that the enzyme-linked fluorescent assay system was useful for visualizing extracellular glutamate concentrations at individual layers of the retina [35]. Glutamate release from presynaptic terminals was monitored as an increase in extracellular glutamate concentrations using this method. Regarding electrophysiological recordings, we assessed the activity of presynaptic terminals and the biophysical properties of postsynaptic glutamate receptors to monitor excitatory postsynaptic currents (EPSCs).

Measurement of gonadal hormone concentrations for animal experiments

In women, progesterone and estrogen concentrations in blood change during the menstrual cycle and are high in pregnancy. Under a regular menstrual cycle, concentrations change from 3 to 60 nM for progesterone and from 0.3 to 1.2 nM for estrogen [36]. In pregnancy, progesterone and estrogen concentrations in blood both increase to a maximum of 1 μM [37]. The concentration of testosterone in blood is reportedly <35 nM [36]. Therefore, we investigated the effects of gonadal hormones at 1 μM in the present study.

Enzyme-linked fluorescent assay

Details on the method used are described in our previous study [35]. In this method, extracellular glutamate concentrations were monitored as the fluorescent signal intensity of NADH, which is a product of the catalytic effects of glutamate dehydrogenase (GDH) between glutamate and nicotinamide adenine dinucleotide (oxidized form).

Slice preparation

Eyeballs were enucleated from 8-week-old mice (C57BL/6J) anesthetized by an intraperitoneal injection of pentobarbital (50 mg/kg). Eyes were hemisected and the retinae were isolated from the sclera. Retinae were placed on a PTFE filter (H100A013A, Advantec Toyo) and sliced in HEPES-buffered solution. Sliced retinae (thickness of 200 μm) were maintained in HEPES-buffered solution bubbled with 100% O_2 at room temperature until used. The composition of HEPES (4-(2-hydroxyethyl)-1-piperazine ethanesulfonic acid)-

buffered solution (in mM) was 135 NaCl, 5 KCl, 2 $CaCl_2$, 1 $MgCl_2$, 10 glucose, and 10 HEPES (pH was adjusted to 7.4 with KOH). The composition of high K solution (in mM) was 135 NaCl, 60 KCl, 2 $CaCl_2$, 1 $MgCl_2$, 10 glucose, and 10 HEPES (pH was adjusted to 7.4 with KOH).

Data sampling

Quartz glasses (22 × 40 mm, Matsunami) coated with GDH were used in experiments. GDH-coated quartz glasses were maintained in HEPES-buffered solution at 4 ºC and used within 24 hours.

Sliced retinae were mounted onto GDH-coated quartz glasses placed on an inverted microscope (Nikon, TMD-300). Slices were covered with a PTFE filter (H100A013A, Advantec Toyo) and fixed with an anchor placed on the PTFE filter. The fluorescent signals of NADH excited by LEDs (emission wavelength 365 nm) were sampled through a barrier filter (>470 nm) using the ARGUS/AC system (Hamamatsu Photonics) to an offline computer every 2 minutes. The focus of the objective lens was adjusted to the surface of the quartz glass.

To reduce possible contamination from background signals, slices were superfused with HEPES-buffered solution for 7.5-10 min before the superfusion of HEPES-buffered solution containing 5 mM NAD^+ and 50 μM DL-*threo*-β-benzyloxyaspartic acid (TBOA), an antagonist of glutamate transporters [38], for 5-10 min. Slices were then exposed to HEPES-buffered solution containing one of the gonadal hormones (progesterone, estrogen, or testosterone) or their derivative (pregnenolone sulfate), 5 mM NAD^+, and 50 μM TBOA. All solutions were bubbled with 100% O_2 and perfused at a rate of 1.5 ml/min. The high K solution was applied as a control stimulation to assess the viability of samples. All experiments were performed at room temperature. Gonadal hormones or their derivatives (purchased from Sigma) were dissolved in HEPES-buffered solution containing 0.1% dimethyl sulfoxide.

Data analysis

Data were selected using the same criteria reported in our previous study to avoid contamination by artifacts [35]. To assess the effects of progesterone, estrogen, testosterone, and pregnenolone sulfate at the layer level, the intensity of fluorescent signals was calculated using fluorescent signals for each ROI (Fig. 1A). Statistical analyses were performed using a one-sample *t*-test. Since samples for progesterone did not show a Gaussian distribution, a non-parametric analysis (the Wilcoxon signed-rank test) was used. All statistical tests were performed using Prism 7.0 (GraphPad Software, La Jolla, CA).

Electrophysiological recordings

We followed the method described in our previous studies [39,40].

Procedure for whole-mount preparations

In brief, mice (2 months old, C57BL/6J) were killed by cervical dislocation, both eyes were enucleated and hemisected, and the retinae were isolated from the sclera. The detached retina was maintained in Ringer's

solution (which contained (in mM): 115 NaCl, 5 KCl, 2 $CaCl_2$, 1 $MgCl_2$, 1.1 NaH_2PO_4, 26 $NaHCO_3$, and 20 glucose; pH 7.4, bubbled with 95% O_2 and 5% CO_2) until used. Recordings were performed in Ringer's solution at room temperature.

Recordings of EPSCs from retinal ganglion cells

A whole-mount preparation was placed on the chamber vitreous side up and viewed under a fluorescent microscope (BX50WI, Olympus, Tokyo, Japan). The input resistance of patch pipettes was 8-12 MΩ when filled with Cs^+-based intracellular solution ((in mM) 115 CsCl, 5 QX-314, 0.5 $CaCl_2$, 5 HEPES, 5 EGTA, 5 ATP-3Na, and 1 GTP-1Na; pH was adjusted to 7.3 with CsOH). To avoid contaminated recordings from displaced amacrine cells, cells with a membrane capacitance of <14 pF were excluded from the analysis. The average membrane capacitance and input resistance of recorded cells were 26 ± 8 pF and 43 ± 9 MΩ (mean ± SD), respectively. EPSCs were recorded using a patch clamp amplifier (Axopatch-200B; Axon Instruments, Foster city, CA, USA) at a holding potential of -70 mV after blocking IPSCs in Ringer's solution containing 1 μM strychnine and 100 μM picrotoxin. Data were sampled at 10 kHz after passing through a low-pass filter at 5 kHz using a commercially available program (pCLAMP9; Axon Instruments, Foster city, CA, USA). Progesterone was dissolved in dimethyl sulfoxide (final concentration in Ringer's solution of 0.1%).

Data analysis of EPSCs

Recorded signals were analyzed off-line. Since the contamination of spontaneous EPSCs made the calculation of mean baseline noise difficult, we were unable to identify EPSCs using the calculated mean baseline noise. Therefore, signals with an amplitude >8pA (approximately 5-fold that of the estimated mean baseline noise when the contamination of spontaneous EPSCs was absent) were automatically detected with the commercial program Minianalysis (Synaptosoft, Decatur, GA, USA) in the present study. A whole trace was then visualized to check for the over- or under-detection of events. The timing of EPSC events was defined as the time of an individual EPSC peak. We analyzed the EPSCs of cells when the frequency of EPSCs was >1 Hz. The average frequency, amplitude, rise and decay times, charge transfer of individual EPSCs, and the sum of the charge transfer of EPSCs for 30 seconds in the presence and absence of progesterone were analyzed. Statistical analyses were performed using a paired *t*-test (two-tailed).

Clinical study

Participants and enrollment criteria

We followed up twelve pregnant women in the present study. Informed consent was obtained from all participants, and those who did not grant authorization for the use of their medical records in research were excluded from the analysis. The medical histories of participants were reviewed at the outpatient clinic of the University of Tokyo Hospital. Inclusion criteria for pregnant women were as follows: (1) eyes with a spherical equivalent between -6 diopters and +3 diopters, and (2) eyes with clear ocular media.

Exclusion criteria were the presence of other eye diseases (e.g. chorioretinal atrophy in the macula, glaucoma, and any other retinal disorders) and high myopia (-6.0 diopters or less). None of the participants were diagnosed with central serous chorioretinopathy (CSC). All data were fully anonymized before the assessment of data.

Eye examination

Participants underwent a set of a comprehensive ophthalmological examinations in the 1st, 2nd, and 3rd trimesters and the postpartum period. These examinations included the measurement of best-corrected visual acuity, AL (IOL master, Tomey OA-2000, version 5.4.4.0006; Tomey, Nagoya Japan), and refractive error (KR-8900 version 1.0.7; Topcon Corp., Tokyo, Japan). After image capturing in each study visit, exported OCT (HRA spectralis; Heidelberg Engineering GmbH, Dossenheim, Germany) images were analyzed using custom written software. An automated graph-based method was used to measure retinal thickness.

Measurement of progesterone

Progesterone concentrations were measured in blood samples collected at the 4 stages of gestation (the 1st, 2nd, and 3rd trimesters and postpartum period) according to the manufacturer's instructions (progesterone ELISA kit, Cosmo Bio.).

Measurement of retinal thickness

We separated the retina into 9 regions (Fig. 5A) and measured the thickness of each region (for see Table 2) to assess possible glutamate toxicity. Changes in the thickness of the retina during pregnancy were assessed using the thickness of the fovea and two surrounding concentric regions (the parafovea and perifovea) (Fig. 5B). The thicknesses of the parafovea and perifovea were calculated as the average thickness of 4 regions (temporal, nasal, superior, and inferior).

Statistical analysis

All statistical analyses were conducted using statistical programming language "R" (version 3.1.3; The R foundation for Statistical Computing, Vienna, Austria).

Abbreviations

CSC: central serous chorioretinopathy, CRT: central retinal thickness, TBOA: DL-*threo*-β-benzyloxyaspartic acid, GDH: glutamate dehydrogenase, HEPES: 4-(2-hydroxyethyl)-1-piperazine ethanesulfonic acid, NADH: nicotinamide adenine dinucleotide (reduced form), NAD^+: nicotinamide adenine dinucleotide (oxidized form), ROI: region of interest, OS: the outer segment of photoreceptors, ONL: the outer nuclear layer, OPL: the outer plexiform layer, INL: the inner nuclear layer, IPL: the inner plexiform layer, GCL: the ganglion cell layer, RGC: the retinal ganglion cell

Declarations

Acknowledgments

This work was supported by Novartis Pharma Research Grants to M. Kaneda, and by JSPS KAKENHI Grant Number JP20K09838 to M. Ohkuma.

Author Contribution

M. Ohkuma, E. Miyachi, and M. Kaneda conducted the experiments of enzyme-linked fluorescent assay. T. Maruyama, T. Ishii conducted the experiments of patch clamp. N. Igarashi, T. Inoue, K. Azuma, and R. Obata conducted the clinical experiments. M. Ohkuma, T. Maruyama, T. Ishii, N. Igarashi, T. Inoue and M. Kaneda prepared the figures. T. Ishii, and M. Kaneda wrote the main manuscript text. M. Ohkuma, T. Ishii, N. Igarashi, and M. Kaneda designed the experiments.

References

1. Compagnone, N. A. & Mellon, S. H. Neurosteroids: biosynthesis and function of these novel neuromodulators. *Frontiers in neuroendocrinology*, **21**, 1–56 (2000).
2. Luine, V. N. Estradiol and cognitive function: past, present and future. *Hormones and behavior*, **66**, 602–618 (2014).
3. Joshi, S. & Kapur, J. Neurosteroid regulation of GABAA receptors: A role in catamenial epilepsy. *Brain research*, **1703**, 31–40 (2019).
4. Guennoun, R. Progesterone in the Brain: Hormone, Neurosteroid and Neuroprotectant.*International journal of molecular sciences.***21** (2020).
5. Shanmugam, A. K. *et al.* Progesterone Receptor Membrane Component 1 (PGRMC1) Expression in Murine Retina. *Current eye research*, **41**, 1105–1112 (2016).
6. Swiatek-De Lange, M. *et al.* Membrane-initiated effects of progesterone on calcium dependent signaling and activation of VEGF gene expression in retinal glial cells. *Glia*, **55**, 1061–1073 (2007).
7. Sakamoto, H., Ukena, K. & Tsutsui, K. Activity and localization of 3beta-hydroxysteroid dehydrogenase/ Delta5-Delta4-isomerase in the zebrafish central nervous system. *The Journal of comparative neurology*, **439**, 291–305 (2001).
8. Nuzzi, R., Scalabrin, S., Becco, A. & Panzica, G. Gonadal Hormones and Retinal Disorders: A Review. *Frontiers in endocrinology*, **9**, 66 (2018).
9. Nuzzi, R., Scalabrin, S., Becco, A. & Panzica, G. Sex Hormones and Optic Nerve Disorders: A Review. *Frontiers in neuroscience*, **13**, 57 (2019).
10. Kwon, H. J. *et al.* Gender Differences in the Relationship between Sex Hormone Deficiency and Soft Drusen. *Current eye research*, **42**, 1527–1536 (2017).

11. Chaychi, S., Polosa, A. & Lachapelle, P. Differences in Retinal Structure and Function between Aging Male and Female Sprague-Dawley Rats are Strongly Influenced by the Estrus Cycle. *PloS one*, **10**, e0136056 (2015).
12. Siesky, B. A. *et al.* Comparison of visual function and ocular hemodynamics between pre- and post-menopausal women. *European journal of ophthalmology*, **18**, 320–323 (2008).
13. Nkiru, Z. N. *et al.* Visual acuity and refractive changes among pregnant women in Enugu, Southeast Nigeria. *J Family Med Prim Care*, **7**, 1037–1041 (2018).
14. Pizzarello, L. D. Refractive changes in pregnancy. Graefe's archive for clinical and experimental ophthalmology = Albrecht von Graefes Archiv fur klinische und experimentelle Ophthalmologie. 241, 484-488(2003).
15. Rao-Mirotznik, R., Buchsbaum, G. & Sterling, P. Transmitter concentration at a three-dimensional synapse. *Journal of neurophysiology*, **80**, 3163–3172 (1998).
16. Roche, S. L. *et al.* Progesterone Attenuates Microglial-Driven Retinal Degeneration and Stimulates Protective Fractalkine-CX3CR1 Signaling. *PloS one*, **11**, e0165197 (2016).
17. Roche, S. L., Wyse-Jackson, A. C., Ruiz-Lopez, A. M., Byrne, A. M. & Cotter, T. G. Fractalkine-CX3CR1 signaling is critical for progesterone-mediated neuroprotection in the retina. *Scientific reports*, **7**, 43067 (2017).
18. Torre, V., Matthews, H. R. & Lamb, T. D. Role of calcium in regulating the cyclic GMP cascade of phototransduction in retinal rods. *Proceedings of the National Academy of Sciences of the United States of America*, **83**, 7109–7113 (1986).
19. Wyse-Jackson, A. C. *et al.* Progesterone analogue protects stressed photoreceptors via bFGF-mediated calcium influx. *The European journal of neuroscience*, **44**, 3067–3079 (2016).
20. Benlloch-Navarro, S. *et al.* Progesterone anti-inflammatory properties in hereditary retinal degeneration. *The Journal of steroid biochemistry and molecular biology*, **189**, 291–301 (2019).
21. Ramirez-Lamelas, D. T. *et al.* Lipoic Acid and Progesterone Alone or in Combination Ameliorate Retinal Degeneration in an Experimental Model of Hereditary Retinal Degeneration. *Frontiers in pharmacology*, **9**, 469 (2018).
22. Allen, R. S. *et al.* Progesterone treatment shows greater protection in brain vs. retina in a rat model of middle cerebral artery occlusion: Progesterone receptor levels may play an important role. *Restorative neurology and neuroscience*, **34**, 947–963 (2016).
23. Jackson, A. C., Roche, S. L., Byrne, A. M., Ruiz-Lopez, A. M. & Cotter, T. G. Progesterone receptor signalling in retinal photoreceptor neuroprotection. *J Neurochem*, **136**, 63–77 (2016).
24. Deschenes, M. C. *et al.* Postmenopausal hormone therapy increases retinal blood flow and protects the retinal nerve fiber layer. *Investigative ophthalmology & visual science*, **51**, 2587–2600 (2010).
25. Getter, T. *et al.* The selective estrogen receptor modulator raloxifene mitigates the effect of all-trans-retinal toxicity in photoreceptor degeneration. *The Journal of biological chemistry*, **294**, 9461–9475 (2019).

26. Kara, N. *et al.* Evaluation of subfoveal choroidal thickness in pregnant women using enhanced depth imaging optical coherence tomography. *Current eye research*, **39**, 642–647 (2014).
27. Sayin, N. *et al.* Subfoveal choroidal thickness in preeclampsia: comparison with normal pregnant and nonpregnant women. *Seminars in ophthalmology*, **29**, 11–17 (2014).
28. Atas, M. *et al.* Evaluation of the macula, retinal nerve fiber layer and choroid in preeclampsia, healthy pregnant and healthy non-pregnant women using spectral-domain optical coherence tomography. *Hypertension in pregnancy*, **33**, 299–310 (2014).
29. Goktas, S. *et al.* Measurement of choroid thickness in pregnant women using enhanced depth imaging optical coherence tomography. *Arquivos brasileiros de oftalmologia*, **77**, 148–151 (2014).
30. Kalogeropoulos, D. *et al.* The physiologic and pathologic effects of pregnancy on the human visual system. *Journal of obstetrics and gynaecology: the journal of the Institute of Obstetrics and Gynaecology*, **39**, 1037–1048 (2019).
31. Akar, Y., Yucel, I., Akar, M. E., Uner, M. & Trak, B. Long-term fluctuation of retinal sensitivity during pregnancy. *Canadian journal of ophthalmology. Journal canadien d'ophtalmologie*, **40**, 487–491 (2005).
32. Sunness, J. S. The pregnant woman's eye. *Survey of ophthalmology*, **32**, 219–238 (1988).
33. Cankaya, C., Bozkurt, M. & Ulutas, O. Total macular volume and foveal retinal thickness alterations in healthy pregnant women. *Seminars in ophthalmology*, **28**, 103–111 (2013).
34. Yildirim, A., Kurt, E., Altinisik, M. & Uyar, Y. Evaluation of retinochoroidal tissues in third trimester pregnants: An optical coherence tomography angiography study.*European journal of ophthalmology*,1120672120966566(2020).
35. Ohkuma, M., Kaneda, M., Yoshida, S., Fukuda, A. & Miyachi, E. Optical measurement of glutamate in slice preparations of the mouse retina. *Neuroscience research*, **137**, 23–29 (2018).
36. Barret, K. E., Barman, S. M., Boitano, S. & Brooks, H. L. chapter 22 Ganong's review of medical physiology (McGraw-Hill Education 2016).
37. Smith, R. *et al.* Patterns of plasma corticotropin-releasing hormone, progesterone, estradiol, and estriol change and the onset of human labor. *The Journal of clinical endocrinology and metabolism*, **94**, 2066–2074 (2009).
38. Hasegawa, J., Obara, T., Tanaka, K. & Tachibana, M. High-density presynaptic transporters are required for glutamate removal from the first visual synapse. *Neuron*, **50**, 63–74 (2006).
39. Ishii, T. & Kaneda, M. ON-pathway-dominant glycinergic regulation of cholinergic amacrine cells in the mouse retina. *The Journal of physiology*, **592**, 4235–4245 (2014).
40. Kaneda, M., Ishii, T. & Hosoya, T. Pathway-dependent modulation by P2-purinoceptors in the mouse retina. *The European journal of neuroscience*, **28**, 128–136 (2008).
41. Lewerenz, J. & Maher, P. Chronic Glutamate Toxicity in Neurodegenerative Diseases-What is the Evidence? *Frontiers in neuroscience*, **9**, 469 (2015).

42. Lambert, S. *et al.* Transient receptor potential melastatin 1 (TRPM1) is an ion-conducting plasma membrane channel inhibited by zinc ions. *The Journal of biological chemistry*, **286**, 12221–12233 (2011).
43. Lesch, A., Rubil, S. & Thiel, G. Activation and inhibition of transient receptor potential TRPM3-induced gene transcription. *British journal of pharmacology*, **171**, 2645–2658 (2014).
44. Majeed, Y. *et al.* Pregnenolone sulphate-independent inhibition of TRPM3 channels by progesterone. *Cell calcium*, **51**, 1–11 (2012).
45. Ciurtin, C. *et al.* TRPM3 channel stimulated by pregnenolone sulphate in synovial fibroblasts and negatively coupled to hyaluronan. *BMC musculoskeletal disorders*, **11**, 111 (2010).
46. Thiel, G. & Rossler, O. G. Hyperforin activates gene transcription involving transient receptor potential C6 channels. *Biochem Pharmacol*, **129**, 96–107 (2017).
47. Thiel, G. *et al.* Pharmacological inhibition of TRPM8-induced gene transcription. *Biochem Pharmacol*, **170**, 113678 (2019).
48. Brown, R. L. *et al.* TRPM3 expression in mouse retina. *PloS one*, **10**, e0117615 (2015).
49. Koike, C. *et al.* TRPM1 is a component of the retinal ON bipolar cell transduction channel in the mGluR6 cascade. *Proceedings of the National Academy of Sciences of the United States of America*, **107**, 332–337 (2010).

Figures

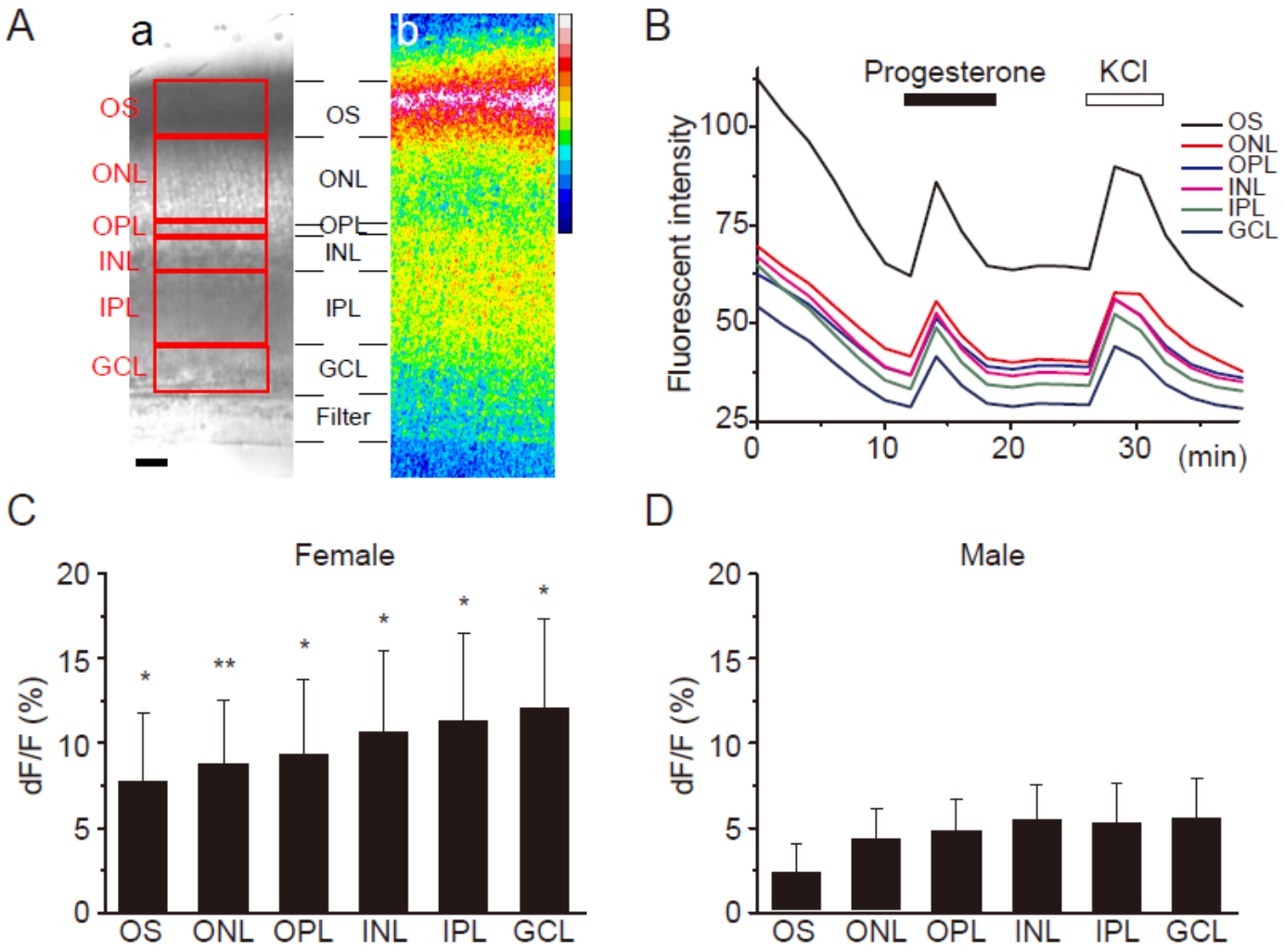

Figure 1

Responses to a progesterone stimulation under the enzyme-linked fluorescent assay system. A. Differential microscopic image of a sliced retina (a) and its pseudo-color image (b). Red-lined rectangles show regions of interest (ROIs). ROIs corresponded to the outer and inner segments of photoreceptors (OS), the cell bodies of photoreceptors (the outer nuclear layer, ONL), the synaptic regions between photoreceptors and second order neurons (the outer plexiform layer, OPL), the cell bodies of second order neurons (the inner nuclear layer, INL), the synaptic regions between second order neurons and ganglion cells (the inner plexiform layer, IPL), and the cell bodies of ganglion cells (the ganglion cell layer, GCL). Filter: filter paper used for preparations (for details, refer to the Methods section). B. Change in the signal intensity to a progesterone or high K stimulation. Data shown were obtained from a female mouse. Bars above the traces show the timing of the application of 1 μM progesterone or 60 mM KCl. C. Change in the signal intensity to a progesterone stimulation in females. The number of samples was 11. D. Change in the signal intensity to a progesterone stimulation in males. The number of samples was 5. * $P < 0.05$, ** $P < 0.01$.

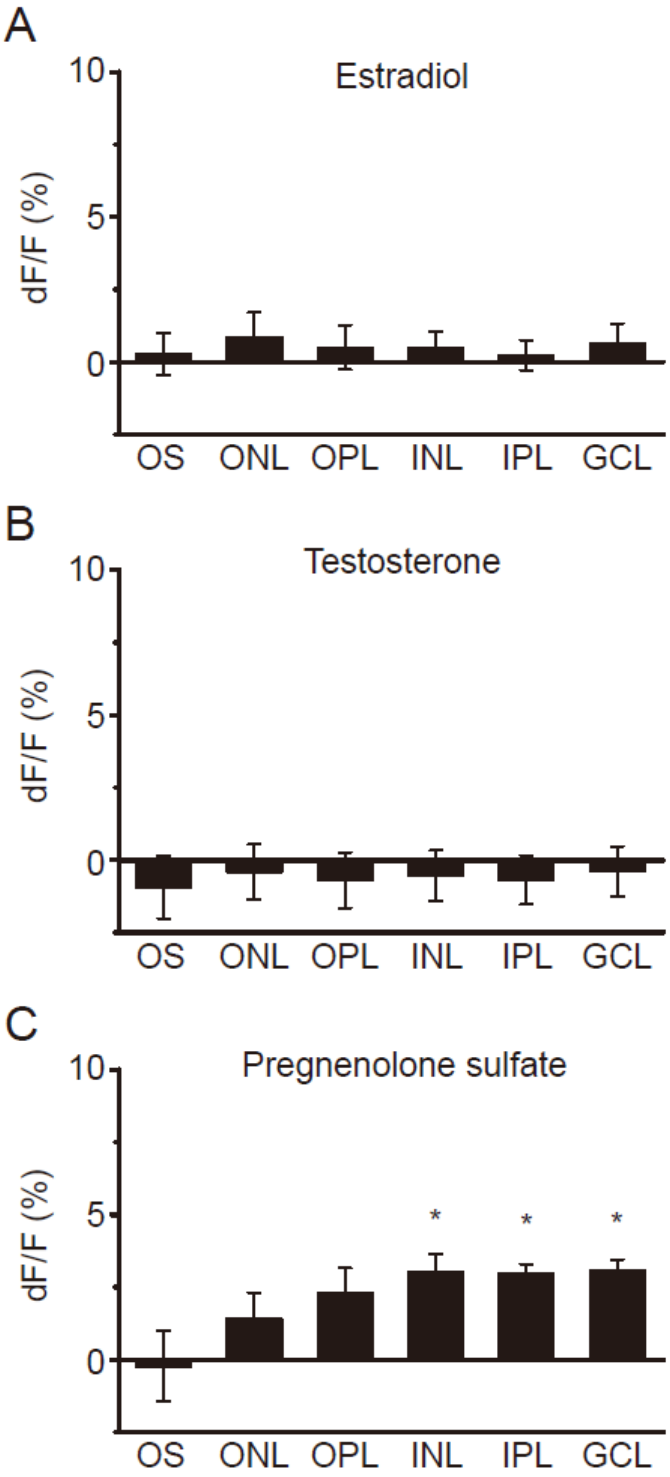

Figure 2

Responses to a 17-β-estradiol (A), testosterone (B), or pregnenolone (C) stimulation using the enzyme-linked fluorescent assay system. The experimental protocol was the same as that shown in Fig. 1. The numbers of samples were 5 for females (estradiol), 5 for females (testosterone), and 3 for females (pregnenolone sulfate). OS, the outer and inner segments of photoreceptors; ONL, the outer nuclear layer;

OPL, the outer plexiform layer; INL, the inner nuclear layer; IPL, the inner plexiform layer; GCL, the ganglion cell layer. * P < 0.05.

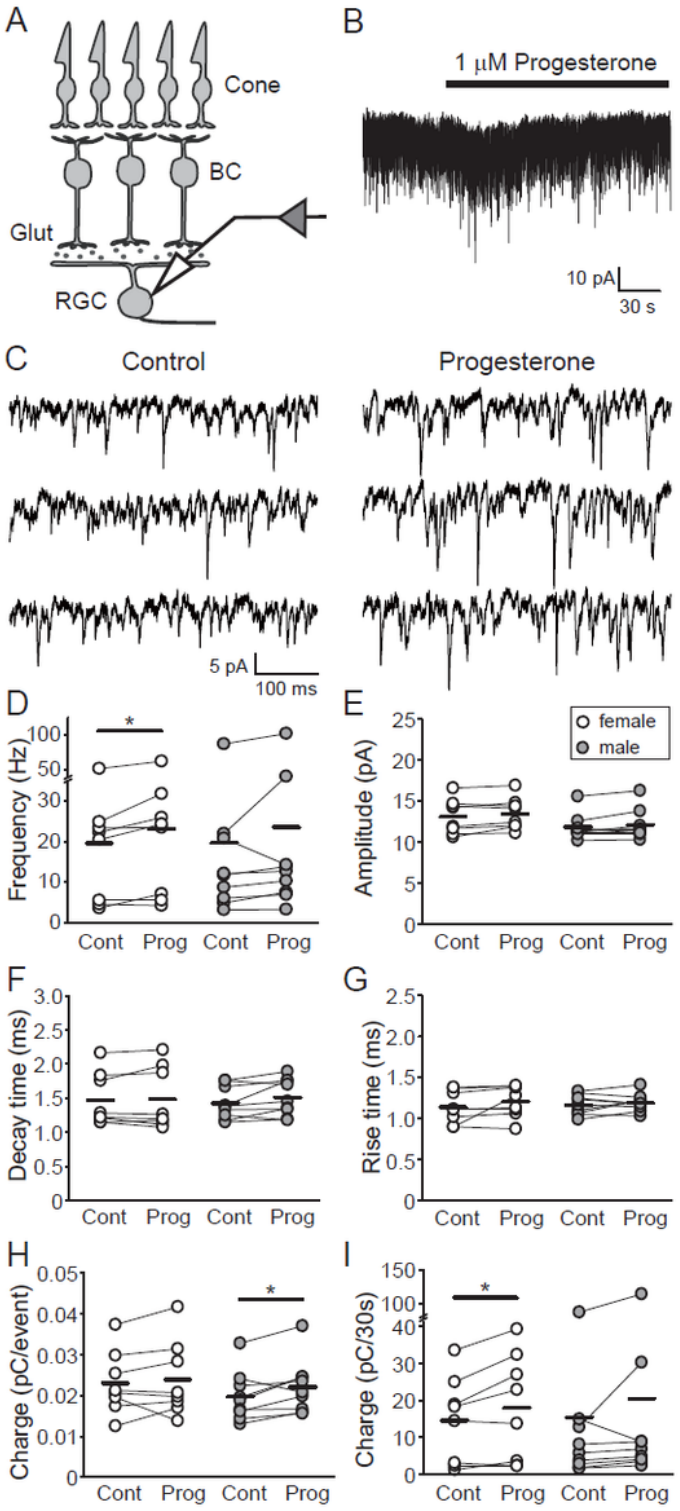

Figure 3

Effects of progesterone on excitatory postsynaptic currents (EPSCs) in retinal ganglion cells. A. Schematic drawings of EPSC recordings. Whole-cell recordings were performed using retinal ganglion cells (RGCs) to monitor EPSCs. Since RGCs receive glutamate (Glut, small gray dots) released from

bipolar cells (BCs), EPSCs recorded from RGCs reflected the activity of glutamatergic synapses between BCs and RGCs. B. Example of a whole-cell recording from an RGC. An RGC was held at -70 mV. Downward sharp lines superimposed on baseline noise correspond to EPSCs. The bar above the trace shows the timing of the application of 1 μM progesterone. C. Enlarged images of EPSCs shown in B. Traces represent before (Control) or during (Progesterone) the application of progesterone. An individual sharp downward deflection corresponds to an individual EPSC. D-I. Effects of progesterone on the parameters of EPSCs. D, frequency; E, amplitude; F, decay time; G, rise time; H, the charge transfer of an individual EPSC; I, the total charge transfer for 30 seconds. Cont, control; Prog, progesterone. Horizontal lines correspond to the mean. The numbers of recorded cells were 9 from 5 male mice and 8 from 4 female mice. *P < 0.05.

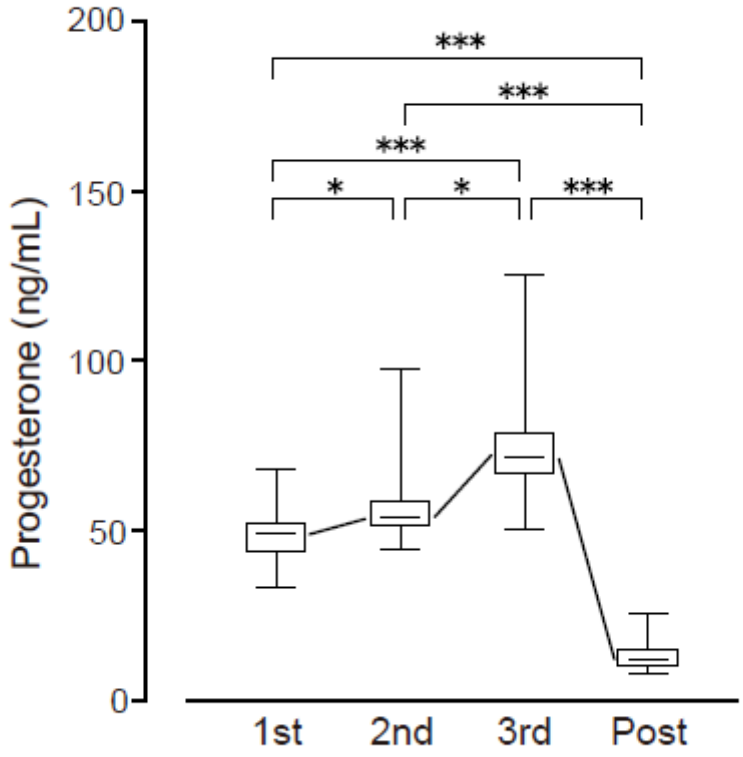

Figure 4

Box plot of progesterone concentrations in 1st, 2nd, and 3rd trimesters and the postpartum period in pregnant women. Whiskers show the maximum and minimum, and box boundaries show the 25th and 75th percentiles. Horizontal lines correspond to the median. * P<0.05, *** P<0.001, the Kruskal-Wallis test. Data were sampled from 12 pregnant women.

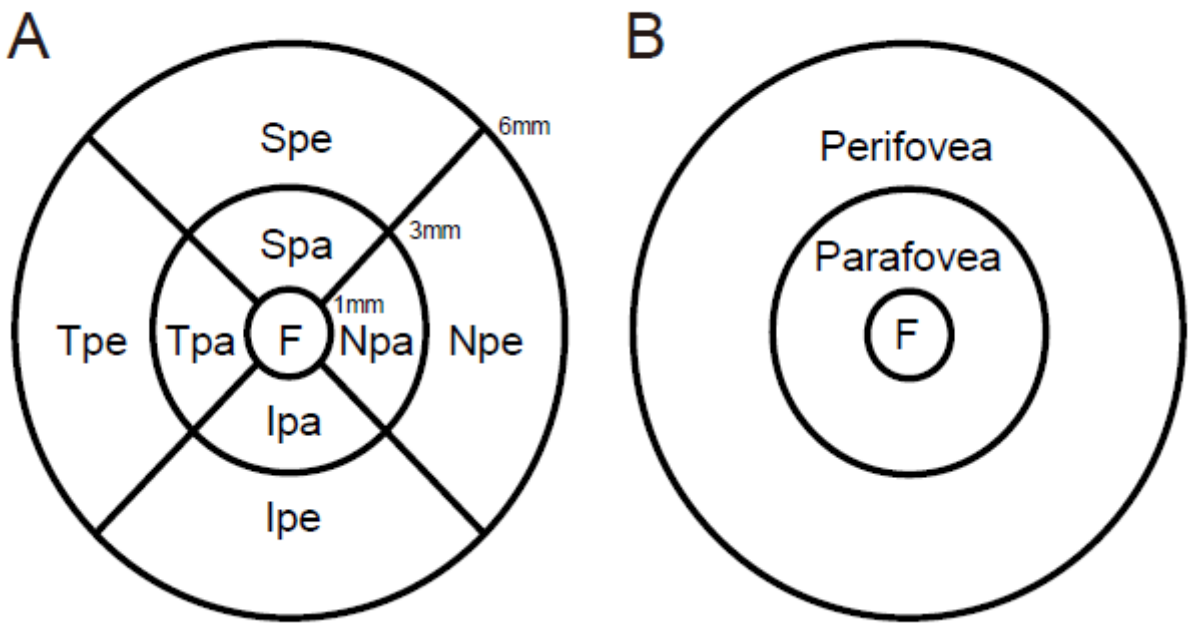

Figure 5

Calculation of retinal thickness. A. Nine regions used for the measurement of retinal thickness. F, fovea; Spe, superior perifovea; Spa, superior parafovea; Tpe, temporal perifovea; Tpa, temporal parafovea; Npe, nasal perifovea; Npa, nasal parafovea; Ipe, inferior perifovea; Ipa, inferior parafovea. B. The central region (fovea) and the two concentric regions (the parafovea and perifovea) used for the assessment of retinal thickness. The thickness of the parafovea used was (Spa + Tpa + Npa + Ipa)/4. The thickness of the parafovea used was (Spe + Tpe + Npe + Ipe)/4.

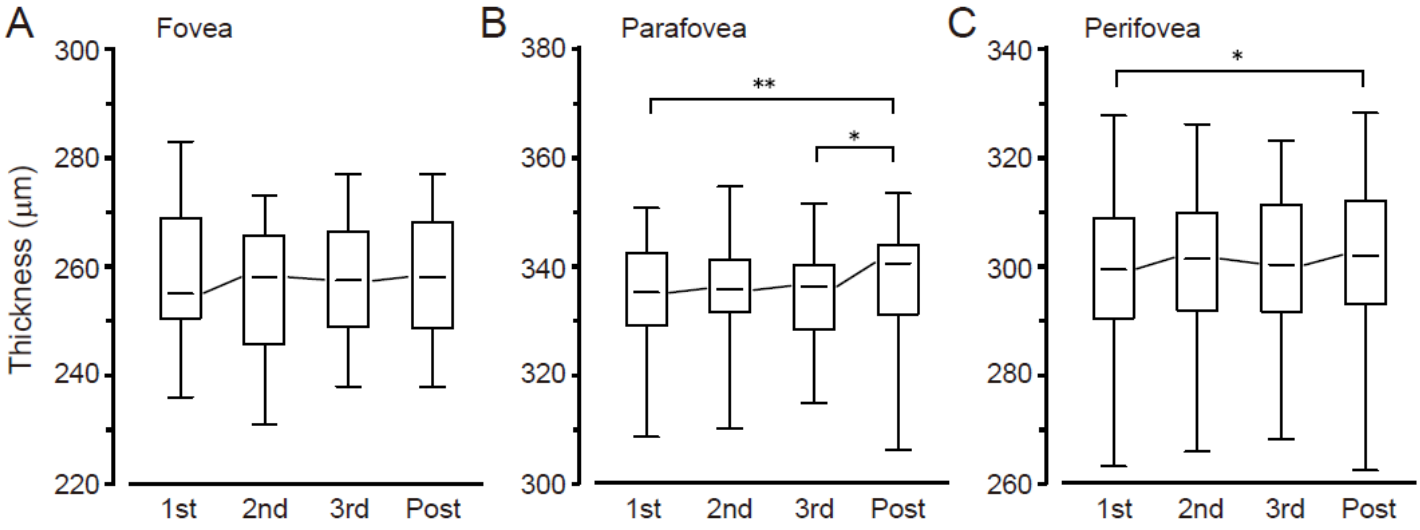

Figure 6

Box plot of retinal thickness in the fovea (A), parafovea (B), and perifovea (C) from 1st, 2nd, and 3rd trimesters and the postpartum period in pregnant women. Whiskers show the maximum and minimum, and box boundaries show the 25th and 75th percentiles. Horizontal lines correspond to the median. Data are the sum of both the right and left eyes of 12 pregnant women (n = 24). * $P<0.05$, ** $P<0.01$. Samples were collected from the right and left eyes of 12 pregnant women (n = 24). Details of the definition of three regions (fovea, parafovea and perifovea) are described in the Methods section.